Reviews

Nanocomposite Materials for Optical Applications

Laura L. Beecroft and Christopher K. Ober*

Department of Materials Science and Engineering, Cornell University, Ithaca, New York 14850

Received August 20, 1996. Revised Manuscript Received May 6, 1997[⊗]

A substantial amount of work has been carried out in the area of nanocomposite materials for optical applications. Composites are typically constructed by embedding an optically functional phase into a processable, transparent matrix material. By doing so, the optical properties can be utilized in more technologically important forms such as films and fibers. This review covers many areas of optical composite research to date. Composites with second- and third-order nonlinearities and laser amplification properties are discussed with examples from the recent literature. Other composites, including transparent magnets, may be made using similar structures. The principles used to construct these composites may have important technological applications soon and are therefore summarized in this review.

1. Introduction

As optical materials applications are expanding, the need for novel optically functional and transparent materials increases. These needs range from high performance, all optical switches for future use in optical computing, to hard transparent coatings as protective or barrier layers. In addition to optical needs such as switching and amplification, the materials must be integrated into existing structures such as waveguides and optical fibers. As such, films and fibers are of great interest as the final form of these novel materials. Nanocomposite materials show great promise as they can provide the necessary stability and processability for these important applications.

The general principles in the construction of optical composites involve the intimate mixing of optically functional materials within a processable matrix. Figure 1 shows this type of composite schematically, where the small particles possess the desirable optical properties and the enclosing matrix imparts processability in film or fiber forms. Examples of incorporated phases include quantum-confined semiconductors, solid-state lasers, small molecules, and polymers. Matrix materials can be polymers, copolymers, polymer blends, glasses, or ceramics. Using such a composite structure, nanocomposites have been formed with nonlinear optical (NLO) and laser amplification properties, among others.

Optical scattering must be avoided in these types of composites, resulting in a tradeoff between particle size and refractive index (RI) mismatch (the difference in RI between the matrix and the particles). For very small particles (typically <25 nm), the RI mismatch is not important, but for larger particles the RI of the matrix and the particles must be carefully matched to avoid scattering. In our work, calculations based on Rayleigh scattering have shown that particles as large as 100 nm require matrix materials with closely matched RI (within 0.02).[1]

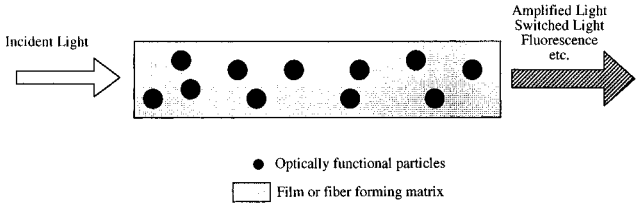

Figure 1. Schematic of optical composite.

Nanocomposite structures have been used to create optically functional materials. By incorporating semiconductor nanoparticles into polymer, glass, or ceramic matrix materials, many of their interesting optical properties including absorption, fluorescence, luminescence, and nonlinearity may be studied. In these systems, very small particle sizes enhance the optical properties while the matrix materials act to stabilize the particle size and growth. Ceramic nanoparticles of solid-state laser materials can be incorporated into polymer matrix materials resulting in laser-active composites. This structure allows the formation of solid-state laser amplifying films which would traditionally be very difficult to make. Optically functional small molecules and polymers may also be included in polymer and glass matrixes and retain their optical properties. Other applications of nanocomposite structures have resulted in transparent materials with unusually high RI, magnetic properties, and excellent mechanical properties.

Nanocomposite structures provide a new method to improve the processability and stability of materials with interesting optical properties. The applications of such composites are extremely broad, ranging from solid-state amplifier films to transparent magnets. This review focuses on recent developments in the synthesis and applications of optical composite materials.

2. Nonlinear Optical Composites

Nonlinear optical materials can be useful for all optical switching and wavelength manipulation. χ^2, or

[⊗] Abstract published in *Advance ACS Abstracts,* June 15, 1997.

S0897-4756(96)00441-3 CCC: $14.00

Table 1. Third-Order Nonlinear Optical Properties in Nanocomposite Materials

	composite	measd NLO strength	units	part of χ^3 measd[a]	λ (nm)	ref
1	CdS in Nafion	-6.1×10^{-7}	cm^2/W	$Im(\chi^3)/\alpha$	480	2
2	CdS in Nafion/NH_3	-8.3×10^{-7}	cm^2/W	$Im(\chi^3)/\alpha$	450	3
3	capped CdSe in PMMA	1.2×10^{-5}	cm/W	$Im(\chi^3)$	544−560	4
4	CdS_xSe_{1-x} glass	1.3×10^{-8}	esu	$[Re(\chi^3)^2 + Im(\chi^3)^2]^{0.5}$	532	6
5	CdS in sol−gel glass	5×10^{-12}	esu·cm	$[Re(\chi^3)^2 + Im(\chi^3)^2]^{0.5}/\alpha$	380	7
6	PPV in SiO_2	3×10^{-10}	esu	$[Re(\chi^3)^2 + Im(\chi^3)^2]^{0.5}$	602	8
7	PPV in V_2O_5	6×10^{-10}	esu	$[Re(\chi^3)^2 + Im(\chi^3)^2]^{0.5}$	602	8
8	GaAs in Vycor glass	-5.6×10^{-12}	cm^2/W	$Re(\chi^3)$	1064	9
		Standard NLO Materials				
9	fused quartz	8.5×10^{-14}	esu	$Re(\chi^3)$	1064	10
10	SF_6	8×10^{-13}	esu	$Re(\chi^3)$	1064	10
11	CdS	-5×10^{-11}	esu	$Re(\chi^3)$	610	5

[a] α is the absorption coefficient.

second-order nonlinear optical materials, can be useful for frequency doubling and optoelectronic switching. By incorporating these materials into composites the stability of χ^2 processes can be improved as shown in section 2.2.3 χ^3, or third-order nonlinear optical materials, can be useful for all optical switching and signal processing. The strength of the nonlinearity can be enhanced by using particles exhibiting quantum confinement effects which can be stabilized by a composite structure. Much work in the area of colloidal semiconductors has focused on taking advantage of this enhancement.

The third-order nonlinear properties of solids are typically reported as the nonlinear susceptibility (χ^3, esu), the nonlinear refractive index (n_2, cm^2/W), or the nonlinear absorption coefficient (α_2/α_0, cm^2/W). Table 1 summarizes nonlinear optical properties for the optical composites that will be discussed in this section. A wide range of χ^3 values have been reported, and large susceptibilities have been shown for several systems.

The nonlinear susceptibility (χ^3) is a complex number (both real and imaginary parts), making comparisons between different measurement techniques difficult. The best strategy is to compare similar measurements, as the conversion between real and imaginary χ^3 can be complicated. Additionally, the susceptibility will change depending on the measurement wavelength. The wavelength may be near or far from resonance, and it will affect the amount of absorption (imaginary contribution to χ^3) in the sample.

Entries 1−3 in Table 1 can be compared to each other as they are all based on nonlinear absorption measurements.[2−4] They can also be compared to the nonlinear absorption of bulk CdS (3.2×10^{-9} cm/W at 610 nm), which is considered to have a strong nonlinear response.[5] Entries 4−7 were all measured using degenerate four-wave mixing experiments, which give the susceptibility as the square sum of the real and imaginary parts.[6−8] The experiment used to measure entry 8 resulted in the nonlinear refractive index, or real part of χ^3.[9] Finally, entries 9−11 in Table 1 show the real part of χ^3 for several commonly studied nonlinear optical materials.[5,10] Quartz has a weak nonlinear response, while bulk CdS is considered to be strongly nonlinear.

All composite values in Table 1 show larger or comparable nonlinear susceptibilities to bulk CdS. The best results have been seen with quantum-confined CdS_xSe_{1-x} (entries 1−4). CdS grown in situ in an ion-exchange resin (section 2.1.2), CdSe grown ex situ using a capping method (section 2.1.4.2), and CdSSe in commercial glass (section 2.1.3.1) all show excellent nonlinear behavior. Composites containing nonlinear optical polymer inclusions have also shown strong nonlinearity (entries 6 and 7, section 2.2.1). Other composites studied show nonlinearities similar to bulk CdS.

Many reviews concerning the synthesis, nonlinear optical properties, and applications of colloidal semiconductors have been written.[11−17] Because such a wealth of information exists for colloidal semiconductor materials, this review will focus only on examples where composite structures are utilized to synthesize and process quantum-confined semiconductors. Wang has coauthored several reviews discussing optical composites and mentioning the potential of these materials as optical devices.[18−20]

Boyd and Sipe published several papers that showed theoretically that the composite structure itself should enhance nonlinear optical properties. Calculations for both spherical inclusions[21] as well as layered composites[22] were presented and demonstrated that the enhancement can come when the NLO material is either the inclusion or the host. The theories have been confirmed experimentally using a dense atomic potassium vapor[23] as well as a layered TiO_2/poly(*p*-phenylenebenzobisthiazole) composite.[24]

A significant amount of experimental work has been done with semiconductor containing composites in a variety of matrix materials. Polymers, including homopolymers, block and random copolymers, and polymer blends, as well as glasses and ceramics such as porous glass, zeolite, and sol−gel glass, have improved the stability and processability of quantum-confined semiconductors. Small molecules and polymers with nonlinear optical properties have also been found to be useful for nonlinear optics in composite form. Composites have been characterized for their structure using techniques such as X-ray diffraction and transmission electron microscopy (TEM). More relevant to this review, the optical properties of these nanocomposites including absorption, fluorescence, luminescence, and optical nonlinearity have been investigated.

2.1. Nanocomposites Containing Semiconductors. *2.1.1. Optical Absorption as a Measure of Particle Size and Distribution.* Currently, semiconductor nanocrystals are primarily studied for their enhanced optical properties. These optical properties are directly related to the size and size distribution of the nanocrystals which can be extracted from the optical absorption spectrum. If crystallite sizes are below the Bohr radius of both the holes and electrons in the semiconductor, strong quantum confinement occurs.[25] Table 2 lists the maximum diameter for strong confinement for several

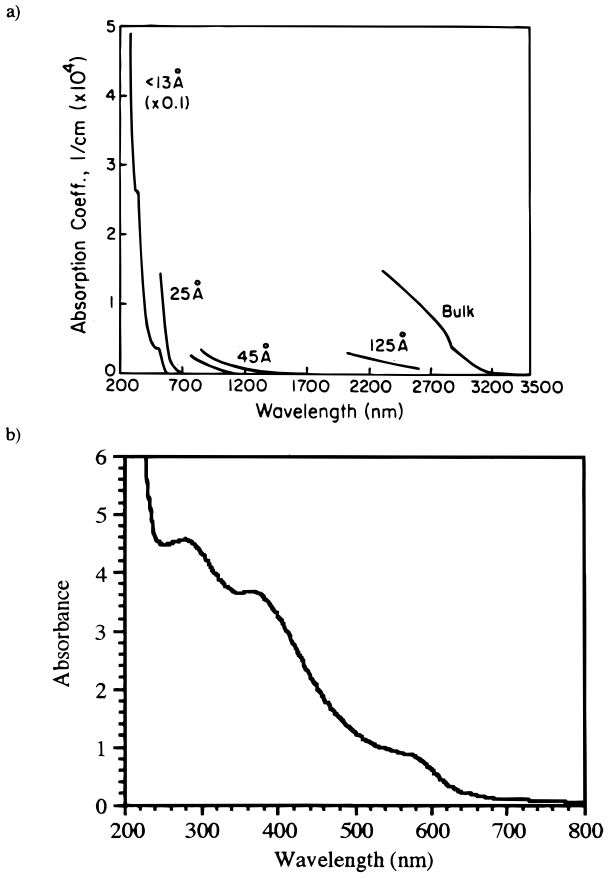

Figure 2. (a) Absorbance spectra shifts as a function of particle size. Reprinted with permission from ref 28. (b) Absorbance spectrum with exciton features from PbS in PVA.

Table 2. Maximum Crystallite Size for Strong Confinement in Several Semiconductors

semiconductor	max diam (nm)	semiconductor	max diam (nm)
CdS	0.9	PbSe	46
PbS	20	GaAs	2.8
CdSe	2	CuCl	0.3

common semiconductors.[26,27] Weaker confinement effects can be seen at somewhat larger crystal diameters. The confinement effect appears as a shift to lower wavelengths in the absorption spectrum representing a changing bandgap. Ideally this shift should be accompanied by exciton features in the spectrum, which show that the particle size distribution is very narrow. The absorption shift and spectral features can act as a measure of particle size and size distribution. Control of these parameters is extremely important in the enhancement of χ^3 effects.

The shift in absorption is illustrated in Figure 2a, which shows a blue-shift with decreasing PbS nanocrystallite size as well as a steepening of the absorption edge for a PbS/polymer composite.[28] Spectra of crystals above 25 Å are featureless, but those below 13 Å show some structure indicating a narrow size distribution in the sample. The smallest particles exhibit a bandgap of 2.3 eV, considerably shifted from the bulk value of 0.41 eV. Figure 2b displays an absorption spectrum with strong exciton features of PbS in poly(vinyl alcohol) made in our laboratories following a modified procedure of Nenadovic et al.[29] The strong exciton features indicated a narrow particle size distribution. The magnitude of the bandgap shift has been correlated with particle sizes of 4 nm,[29] although the shift is at a slightly lower wavelength than that shown for 4.5 nm particles in Figure 2a.

Alivisatos et al. studied the homogeneous and inhomogeneous contributions to the optical spectrum of CdSe nanocrystals using optical hole burning.[30] The CdSe clusters were synthesized using inverse micelles and redispersed in polystyrene for the optical measurements. The inhomogeneous contributions, caused by even small variations in size distribution, dominated the spectra. Because of this inhomogeneous broadening, the size distribution must be carefully controlled to maximize quantum effects. As will be shown throughout the semiconductor examples, size distribution control is often quite difficult with these quantum-confined materials.

Early absorption measurements showed either little shift in absorption edges[31] or no exciton features when the edges were shifted.[32] Copolymers containing polyethylene (85%) and poly(methacrylic acid) (15%) aided the synthesis of PbS-containing composites prepared by Wang et al.[28,33] The particle sizes could be altered by changing the concentration of Pb^{2+} in the films and by subsequent heat treatments. Bandgap and absorption measurements were made over a range of crystallite sizes (Figure 2a), and theoretical models were used to explain the trends of the data.

Work with poly(vinyl alcohol) as a stabilizer and matrix material for PbS has consistently shown shifted and featured absorption spectra (Figure 2b). This was first observed by Gallardo et al. in 1989 in a study of the absorption and fluorescence properties.[34] Nenadovic et al. also studied similarly prepared materials with particular interest in the effects of surface properties on the bleaching of PbS.[29] Our group has also carried out some research in this area, improving the film-forming nature of the composites.[35]

2.1.2. Semiconductor Composites with Polymer Matrix Materials. Early work with quantum-confined semiconductors was performed in colloidal solutions,[36−38] which could often be stabilized with small amounts of polymer.[39] After several years of work with polymeric stabilizers, these stabilizers were discovered to be excellent matrix materials yielding processable polymer films with semiconductor optical properties. The resulting films often were more stable than colloidal solutions and were useful for many optical measurements.

The first group to formally recognize semiconductor polymer composites such as these in terms of engineered optical media was Akimov et al. in 1992.[40] In this work, CdS nanocrystals from 2 to 50 nm in size were prepared in poly(vinyl alcohol), poly(vinylpyridine), and photographic gelatin. Other polymers that did not stabilize the particles were also mentioned. Remarkably high CdS concentrations, up to 50 wt %, could be prepared without agglomeration. The composites exhibited good photosensitivity and photoconductivity. Particular applications of interest to the authors included dispersive optical elements, bandpass and cutoff filters, and electrophotographic and photothermoplastic materials.

The earliest semiconductor composites were used for their catalytic properties rather than their optical properties.[41] Early in the catalysis work, in situ synthesis methods were developed by Krishnan et al.[42] By

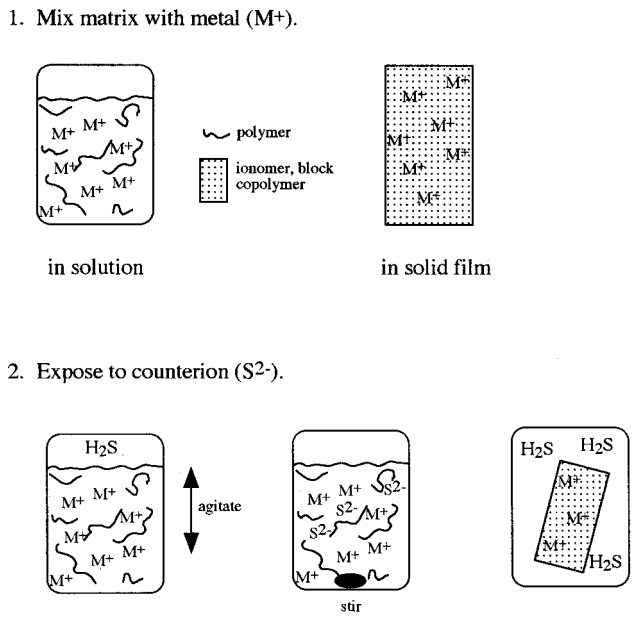

Figure 3. Schematic of in situ polymer synthesis methods.

ion exchanging a Nafion matrix (perfluoroethylenesulfonic acid ion-exchange polymer) with Cd^{2+}, then exposing to H_2S, submicron particles were produced, which could photocatalytically drive chemical reactions. Mau et al. used a similar method that created 20 nm size particles which were used for photocatalytic hydrogen generation in the presence of platinum catalyst.[43] These in situ methods were later utilized for the novel optical properties that could be generated.

The general scheme used to prepare polymer−semiconductor composites in situ is shown in Figure 3. In a typical experiment, the matrix material and metal ions are mixed in solution and are then exposed to the counterion (S^{2-}, Se^{2-}) in the form of gas or as ions dissolved in solution. The composite may be cast as a film before or after exposure to the counterion. For example, if poly(vinyl alcohol) (PVA) were the matrix material for PbS nanoparticles, a solution of PVA and Pb^{2+} could be prepared in water (step 1a). This solution could then be exposed to H_2S gas in order to form the PbS and then cast as a film (step 2a). In this particular reaction, the crystalline semiconductor forms extremely quickly yielding a wine-red solution. Similarly, if a block copolymer were to be used as the matrix, Pb^{2+} could be complexed with the copolymer in solution and then cast as a film (step 1b). The phase-separated film, which might require annealing, would then be exposed to H_2S gas in a closed container (step 2c). Over a period of several hours, the film would turn brown, indicating PbS formation. Many variations in this general synthesis scheme can be imagined.

2.1.2.1. NLO Properties of Polymer Composites. While most authors praise the enhanced nonlinear optical properties of quantum confined semiconductors, few actually have measured them. Wang et al. at DuPont have been the leaders in making these measurements on polymeric systems. In 1987, Wang and Mahler reported the first study of NLO properties in polymer stabilized quantum-confined semiconductors using the degenerate four-wave mixing (DFWM) results of a CdS/Nafion composite.[44] The particles studied were 50 Å in size, which would cause moderate confinement (Table 2) and resulted in a bandgap of 2.55 eV (the bandgap of

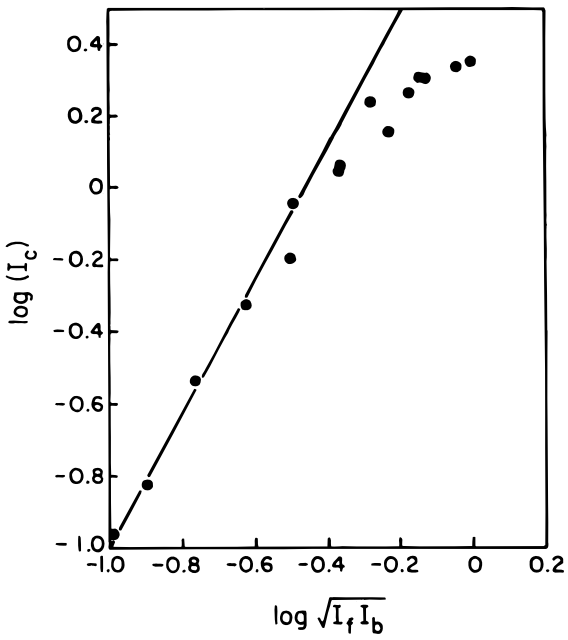

Figure 4. Nonlinear optical properties in a CdS/polymer nanocomposite. Reprinted with permission from ref 44.

bulk CdS is 2.5 eV). DFWM measurements were taken at 505 nm (2.43 eV) as shown in Figure 4, where a slope of 1.9 and saturation at about 2 MW/cm^2 were found, indicating a third-order process. The signal strength was about half that seen in semiconductor-doped glass samples, and a 10 ns response time was measured. The saturation indicated that a three-level saturable absorber model was the most likely mechanism for nonlinearity in these composites. A later paper reported DFWM experiments and absorption saturation experiments that confirmed the interesting nonlinear optical properties of these composites.[45]

Hillinski et al. presented work concerning 5.5 nm CdS clusters grown in Nafion, with a focus on the NLO properties.[2] Their films showed large χ^3 nonlinearity ($\alpha_2/\alpha_0 = -6.1 \times 10^{-7}$ cm^2/W) which they attributed to the bleaching of the exciton absorption. This bleaching was enhanced due to the high concentration of surface defects on the small particles. They cautioned that an understanding of the surface chemistry of these particles will be very important in the interpretation of their properties.

Continuing this work, Wang et al. further discussed bleaching of quantum-confined CdS particles in Nafion films.[3] Crystallites in a range of sizes up to 40 Å were synthesized and passivated with ammonia. The effects of surface-trapped, electron−hole pairs were examined using absorption, photoluminescence, and pump−probe experiments. An even higher χ^3 nonlinearity ($\alpha_2/\alpha_0 = -8.3 \times 10^{-7}$ cm^2/W) was measured in the surface passivated samples. A short review paper by the same group reported the NLO properties for the CdS in Nafion samples.[46]

Nonlinear optical measurements were also made on CdS grown in a swollen, cross-linked, copolymer matrix.[47] A third harmonic generation experiment was used, comparing intensities to a quartz reference. Near resonance at 1.45 μm, an increase in signal as much as 11.2 times the reference was observed. Off resonance at 1.06 and 1.5 μm small increases from 1.2 to 1.6 times the quartz standard were shown.

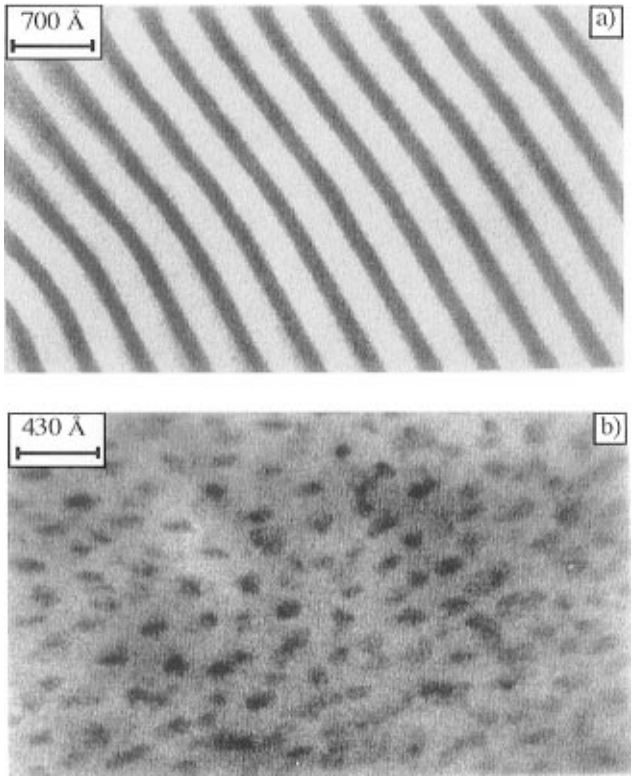

Figure 5. TEM micrographs of ZnS in a block copolymer. (a) Lamellar morphology, (b) spherical morphology. Reprinted with permission from ref 52.

2.1.2.2. Using Polymer Architecture To Control Particle Size. As has been mentioned, particle size and size distribution must be carefully controlled in order to take advantage of NLO enhancement effects. The architecture of the polymer matrix can be used to help in controlling these parameters. Both block copolymers and polymer blends exhibit phase separation, which may help isolate the semiconductor clusters as they form. In some cases this controlled phase separation can result in superlattice structures. Most work in the area of superlattices have been with colloidal solids;[48,49] however, similar structures may be possible with composites.

Researchers at MIT have done extensive work with block copolymers prepared using the ring-opening metathesis polymerization (ROMP) synthesis technique. By taking advantage of the phase separation of the block copolymers, good stabilization of the semiconductor was found. STEM studies of PbS[50] as well as CdS and ZnS[51] composites showed that small particles can be synthesized utilizing spherical phase separation of the metal-containing phase; however, the optical properties were not measured. The bandgap of 30 Å ZnS particles prepared by this technique was 5.7 eV, which is considerably higher than the bulk bandgap of 3.5 eV.

Similar copolymers were synthesized which were used to prepare ZnS- and Zn-containing composites in both lamellar and spherical morphologies.[52] As seen in Figure 5, both lamellar (Figure 5a) and spherical (Figure 5b) morphologies effectively isolated the ZnS particles (dark regions) in a controlled manner. Both morphologies resulted in clusters less than 20 Å in size with a bandgap of 6.3 eV. X-ray and X-ray photoelectron spectroscopy were also used to characterize these materials. In 1994, members from the same research group again reported PbS grown in a ROMP block copolymer.[53] These composites displayed a featured absorption spectrum, indicating a narrow size distribution, but were primarily characterized by TEM and X-ray diffraction.

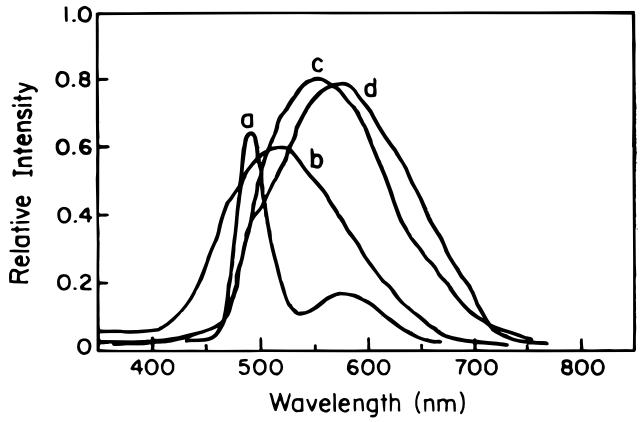

Figure 6. Fluorescence spectra of CdS in several polymer blend compositions. PSP:CA = (a) 1:4, (b) 1:1, (c) 2:1, and (d) 4:1. λ_{ex} = 400 nm. Reprinted with permission from ref 57.

Möller reported the growth of nanocrystals of many semiconductors, including CuS, CdS, and PbS, in block copolymers of polystyrene and poly(vinylpyridine) with spherical morphology.[54] Shifted absorption spectra were shown indicating small particle sizes, but the absorbance spectra were featureless, indicating that the particles were not monodisperse. More recent work by the same group on gold nanoparticles has shown that the stabilization of the ionic block is very important if a single particle per micelle is desired.[55] When a poly(ethylene oxide) block was used as a matrix for gold particles, heat treatment caused the particles to come together, resulting in a system where the particle size could be controlled by the composition of the copolymer and the concentration of ions. However, when poly(vinylpyridine) was used as the stabilizing block for gold (and several semiconductors) the particles did not coalesce during heat treatment because the stabilization was much stronger. The strategy for forming one particle per micelle using a weakly stabilizing block and heat treatment might be very important if it can be extended to semiconductor particles.

The first work utilizing polymer blends as matrix materials was reported by Yuan et al.[56,57] Quantum-confined CdS was prepared in poly(styrene phosphonate diethyl ester) (PSP) and cellulose acetate (CA) polymer blends, resulting in structured absorption spectra. The phosphonate ester chelates metal nitrates, isolating them before reacting with H_2S. The fluorescence results, shown in Figure 6 for several PSP:CA compositions, showed a shift to lower energies with increasing amounts of PSP. This behavior indicated increasing particle sizes with increasing PSP composition. The particle sizes measured by absorbance edge position were 44 Å (Figure 6a, 2.81 eV), 58 Å (Figure 6b, 2.63 eV), and 82 Å (Figure 6d, 2.48 eV). The higher energy peak in Figure 6a may be due to excitonic fluorescence or due to crystalline cellulose acetate being present. Continued work showed size quantization by the changing bandgap and structured absorption spectra.

2.1.3. Semiconductor Composites with Inorganic Matrix Materials. A significant amount of work in the area

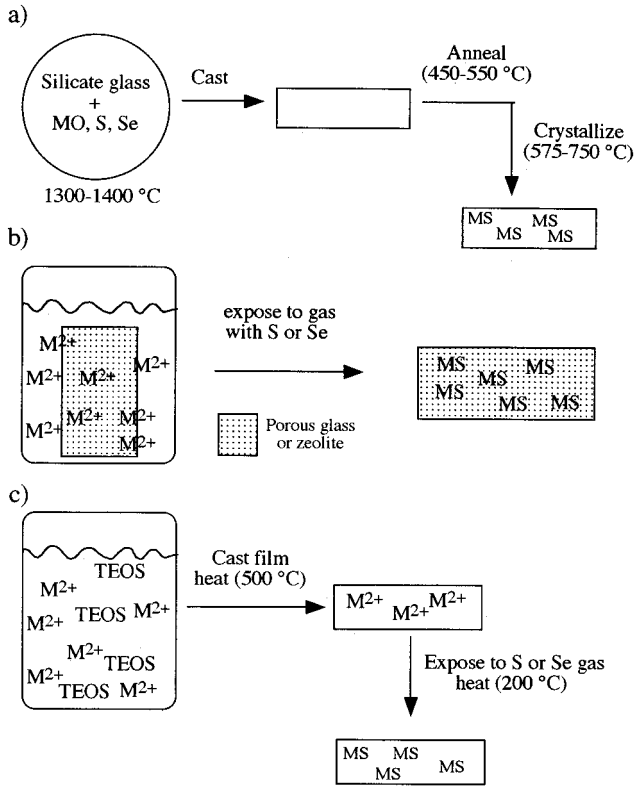

Figure 7. Schematic of semiconductor nanocomposite synthesis in glass and ceramic matrixes. (a) Traditional glass, (b) porous glass or zeolite, (c) sol−gel glass.

of quantum-confined semiconductors has been carried out with high-temperature glass, porous glass, zeolite, and sol−gel derived matrix materials. The small and regular pore sizes of these materials are useful in controlling the particle sizes and distributions of the semiconductor nanoparticles. Additionally, semiconductor/semiconductor composites have been found to have enhanced optical properties. Early work in this area was done on commercially available CdS_xSe_{1-x} glasses which are used as sharp-cutoff color filters. Large size distributions and varying sulfur concentrations made these materials difficult to study quantitatively. More recent work deals with precisely synthesized compositions. Figure 7 summarizes the synthesis of nanocomposites in various glass and ceramic structures.

2.1.3.1. High-Temperature Glasses. Synthesis of semiconductors in glasses involves the incorporation of the necessary ions in the glass at high temperature, casting to form a monolith, annealing to remove stresses, and heat treatment to crystallize the semiconductor as shown in Figure 7a. Nonlinear optical measurements were made very early in the work with glass nanocomposites. In 1983, Jain and Lind studied degenerate four-wave mixing in commercial CdS_xSe_{1-x} glass, and compared the results to single-crystal CdS.[6] They showed that the glass could be used as an aberration corrector, with χ^3 values as high as 1.3×10^{-8} esu and a fast response time. Warnock and Awschalom showed confinement in these glasses using luminescence experiments.[58] Cullen et al. fabricated directional couplers using ion-exchanged waveguides from similar semiconductor-doped glasses.[59]

Roussignol et al. continued experiments on the glasses used by Jain and Lind.[60,61] In an extensive study, researchers at Corning Inc. reported results concerning

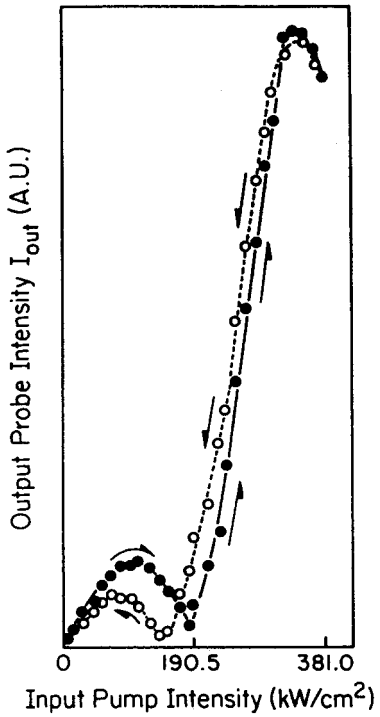

Figure 8. Switching behavior in commercially available CdSSe glass. Reprinted from ref 63.

commercially available filter glasses ($CdSe_xS_{1-x}$) as well as experimental CdS and CdSe glasses.[62] The experimental glasses they studied showed featured absorption and luminescence spectra, indicating small monodisperse particle sizes, which were confirmed by TEM. Other phases such as AgCl and CuCl were grown by similar techniques and resulted in quantum-confined materials.

More recently, the first observation of resonatorless bistability and nonlinear switching due to increasing absorption in a semiconductor-doped glass was reported.[63] A nondegenerate pump−probe technique was used to measure these effects in CdS_xSe_{1-x}-doped glass. Perfect switching behavior could be demonstrated by changing the pump intensity as shown in Figure 8. Input power above 167 kW/cm^2 resulted in a region of high absorption, while below this value the material was very transparent, defining two distinct regions of switching and dephasing. Absorption induced bistability does not require extra resonators such as Fabry−Perot resonators or phase matching elements to create nonlinear switching.

2.1.3.2. Porous Glasses. Porous glasses contain well-defined pores which can assist in confinement of the semiconductor clusters. They are attractive as host materials because low-temperature solution and gas-phase synthesis techniques can be used. Figure 7b shows a typical synthesis procedure where the glass is infiltrated with the metal ions and subsequently exposed to H_2S (or the appropriate counterion) to form the semiconductor nanoparticles. The work of Kuczynski and Thomas discussed CdS prepared in porous Vycor glass.[64] The CdS was confined in only one dimension, giving some excitonic structure to its absorption spectrum, but bandgap properties were similar to bulk CdS. The effects of methylviologen and water on the spectroscopic properties including emission and quenching were studied.

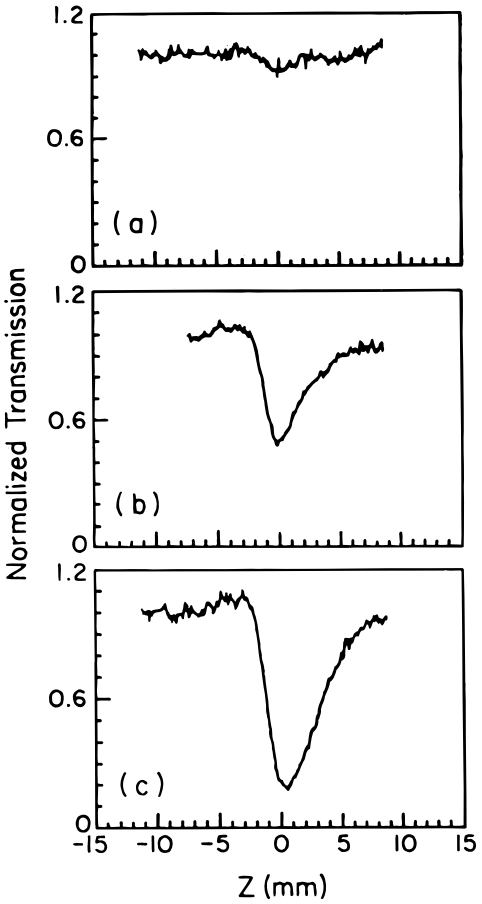

Figure 9. Z-scan data for GaAs-doped Vycor glass. Reprinted with permission from ref 9.

Luong discussed the growth of Cd, Pb, and Zn sulfides and selenides in Vycor glass.[65] For Zn- and Cd-containing crystallites, only a small shift from bulk properties was seen, due to broad particle size distributions and particles larger than the Bohr radius of the exciton. PbS and PbSe showed quantum confinement in the glass with blue-shifted absorption spectra which became structured upon heat treatment.

Justus et al. measured the optical properties of 50 Å GaAs particles grown in Vycor glass.[9] The nonlinear measurements showed n_2 of -5.6×10^{-12} cm^2/W, an order of magnitude stronger than the bulk material. This is shown in the Z-scan data presented in Figure 9, where the nonlinear response increases with increasing power. The valley which develops with increasing intensity indicates nonlinear absorption. The difference in transmission between the maxima and minima is directly related to the change in refractive index. Because the peak of transmission precedes the valley, the response is negative. Measurements were taken in the technologically important near IR region, although this region is far from resonance for GaAs.

2.1.3.3. Zeolites. Zeolites are crystalline ceramics with well-defined pores of uniform size and size distribution. The synthesis of composites based on these materials is quite similar to that of porous glass composites shown in Figure 7b. Unlike porous glasses, the zeolite pores are situated on a lattice so that materials substituted in them might form a superstructure as well as have quantum semiconductor properties. A survey of synthesis techniques is presented by Ozin et al.[26]

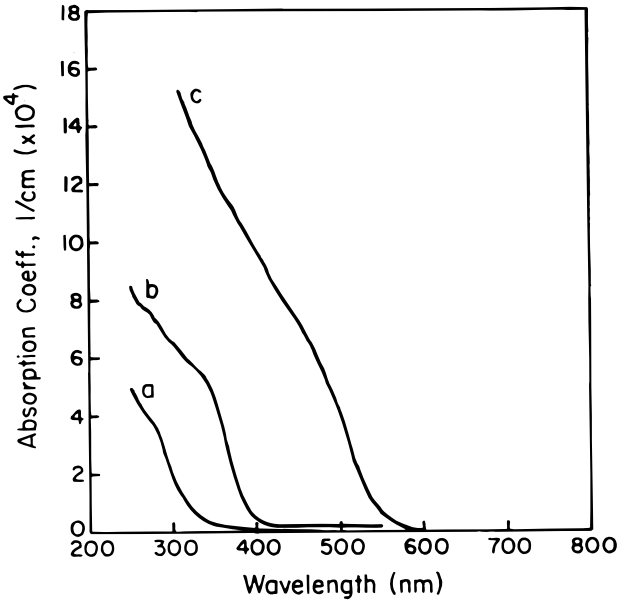

Figure 10. Absorption spectra for CdS in zeolite Y. (a) 1.1 wt % CdS/Y, (b) 7.4 wt % CdS/Y, (c) micron-sized CdS. Reprinted with permission from ref 66.

Wang and Herron presented absorption spectra from CdS and PbS grown in two zeolites.[66] A blue-shifted absorption was found for both semiconductors which shifted to red as the concentration of semiconductor was increased, shown in Figure 10 for a CdS/Zeolite Y composite. Above concentrations of about 4 wt %, the optical shift was abruptly arrested because the percolation threshold of the zeolite was reached, and no change was observed with loading up to 18 wt % and 100 °C heating. No intermediate absorption levels were observed between those shown in the figure. The three-dimensional lattice allowed the synthesis of clusters with solid-state behavior which differs from the bulk.

Later some of the same authors described work concerning CdS clusters grown in other zeolite hosts.[67] As had been seen earlier, the CdS particles remained discreet within the host at low concentration, but above concentrations of 4% a supercluster structure developed. The supercluster structure had optical properties intermediate between the individual clusters and the bulk. The authors indicated the potential of controlling the structure and electronic properties by the choice of zeolite host material.

Wang and Herron reported the luminescence and excited-state dynamics of CdS grown in zeolites X, Y, and A.[68] Three emission bands were found in the yellow-green, red, and blue, which could be attributed to defects. The yellow-green emission was attributed to Cd atoms, while the red and blue were attributed to S-related defects.

Later Möller et al. compared the structure of PbS in two zeolites to PbS in a polymer matrix using extended X-ray absorption fine structure.[69] The PbS was found to be more confined in the zeolite matrix than in the polymer, with higher order at higher concentrations. Considerably larger PbS particles were generated in the polymer matrix.

2.1.3.4. Sol−Gel Derived Glasses. Sol−gel type syntheses allow for low-temperature processing, high purity, and more flexibility in the components of the glass. Additionally, sol−gel precursors lend themselves to film

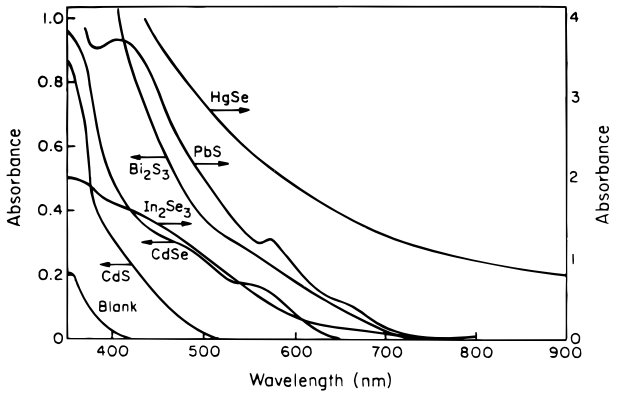

Figure 11. Absorption spectra for several semiconductors prepared in sol−gel glasses. Reprinted with permission from ref 71.

and fiber applications more readily than other glass and ceramic composites that have been discussed. Figure 7c shows this type of synthesis schematically. Typically the sol−gel glass is prepared with the metal ions present and exposed to S^{2-} (or other counterions) after glass formation. Levy and Esquivas give a nice review of the use of sol−gel matrix materials to design optical materials.[70] They discuss CdSe as well as laser dyes and liquid-crystalline materials as incorporated phases, all taking advantage of the small pore sizes of the sol−gel derived materials.

Several semiconductors were incorporated into sol−gel silicate glasses by Rajh et al.[71] The synthesis involved preparing the colloidal semiconductor with a stabilizer (20−40 Å) and then adding tetramethyl orthosilicate to form the matrix. The samples were dried, but not heat treated, and showed shifted and featured absorption for several compositions shown in Figure 11. Some solutions lost exciton features during drying which could be recovered by exposure to H_2S.

Structured and shifted absorbance spectra were seen in CdS nanoparticles in sol−gel glass depending on heat treatment of the glass.[72,73] The crystalline structure of the nanoparticles was confirmed by X-ray diffraction. Othmani et al. discussed the preparation of CdS in sol−gel derived SiO_2 at concentrations up to 20%.[74] X-ray and Raman studies were combined to predict a particle size of about 7 nm. Nogami et al. reported the controlled preparation of CdS_xSe_{1-x} in sol−gel derived SiO_2 glass.[75] Shifted absorption edges and bandgaps varying with particle size were shown, but the absorption spectra were featureless due to large size distributions.

Glasses derived from sol gel precursors for SiO_2 and $1.4Na_2O-20.8ZrO_2-77.8SiO_2$ were used to stabilize in situ growth of CdS crystallites.[7] The sodium glass showed much higher stability to CdS oxidation at high temperatures than the simple SiO_2 glass. Absorption edges were featureless and χ^3 parameters of about 5×10^{-12} esu were measured for several conditions. This synthesis of a mixed oxide glass took advantage of the compositional flexibility of the sol−gel route.

2.1.3.5. Semiconductor Matrix Composites. Thin-film composites have been constructed which contain semiconductor nanoparticles in a semiconductor matrix.[76] The synthesis involves preparation of quantum-confined CdSe and CdSe coated with ZnSe by a colloidal method. The nanoparticles are then dispersed by an electrospray during the organometallic chemical vapor deposition of a ZnSe thin film. Because the bandgap of ZnSe is much higher than CdSe, the nanoparticles are very well isolated from each other. The photoluminescence behavior was measured and showed that nanoparticles that were coated with ZnSe before film formation had much higher efficiency. Composites such as these may be more easily integrated into electronic devices because the conductivity of the matrix can be controlled by doping.

2.1.4. Controlling Particle Size. In all of the semiconductor work discussed here, the size and size distribution of the particles have been of great interest. Particle size and size distribution are critical in maximizing enhancement in quantum-confined systems. The particle size affects the magnitude of the shift in absorption (change in bandgap), while the distribution affects the strength of the quantum effect at a given wavelength. These properties can be controlled by the polymer matrix architecture (2.1.2.2), porous matrix materials (2.1.3), additives and heat treatments (2.1.4.1), and ex situ particle-capping methods (2.1.4.2). Polymer architecture and porous matrix materials have been discussed and typically result in a fixed particle size determined by the matrix structure. Other methods discussed in this section can result in tunable particle sizes which might be particularly useful in changing the wavelength of operation in optical devices.

2.1.4.1. Heat Treatments and Additives. Heat treatments and additives have been coupled with composite synthesis strategies to control particle size and distribution. In the early work of Wang et al., shown in Figure 2a, PbS particle size was controlled by varying the concentration of the Pb^{2+} and heat treating the samples.[28] Similarly, work from the same group on CdS in Nafion (section 2.1.2) also found that heat treatment could be used to control particle size.[3] Sankaran et al. found that ZnS cluster size was increased when the block copolymer films were exposed to H_2S at higher temperatures or in the presence of solvent vapor (section 2.1.4).[52] Annealing after ZnS formation, however, did not result in particle growth probably because the matrix acted as a diffusion barrier. Heat treatments have also been used in many of the glass and ceramic matrix materials discussed previously.[72,73]

Kyprianidou-Leodidou et al. varied the size of PbS in poly(ethylene oxide) from 4 to 80 nm using acid and surfactant additives.[77] Without additives, particle sizes were about 29 nm. Acetic acid increased the particle sizes, while sodium dodecyl sulfate, a surfactant, lowered them. Although the control of average particle size was demonstrated, the size distributions were quite large.

In our work with PbS synthesized in poly(vinyl alcohol) (PVA), attempts were made to change particle sizes using similar treatments.[35] In a standard reaction of PbS in PVA, 4 nm particles were reproducibly synthesized as shown in the absorbance spectrum in Figure 2b. The concentration of the PVA was increased from the standard 0.1% up to 5% in water and found to have no effect on the particle sizes while improving the film-forming abilities and increasing photostability. Acetic acid was added to the synthesis and showed an increase in particle size by X-ray line broadening seen in Figure 12. As shown, the standard reaction produced

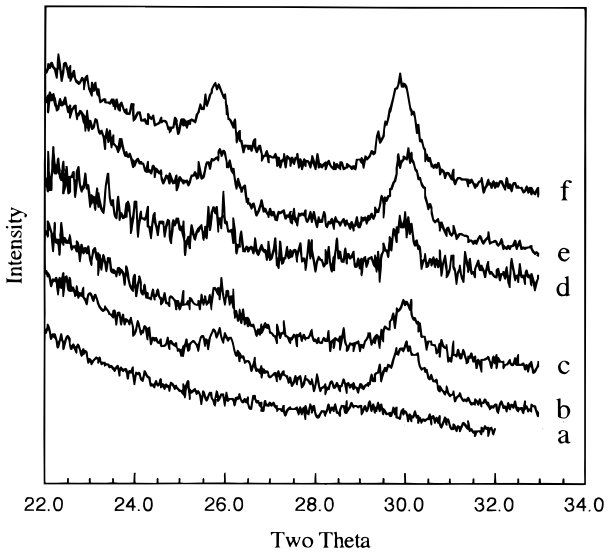

Figure 12. X-ray line broadening due to added acetic acid in the formation of PbS in PVA. (a) No added acid, (b) 0.015 M, (c) 0.076 M, (d) 0.38 M, (e) 0.46 M, (f) 0.53 M.

a particle size (4 nm) which resulted in a featureless spectrum (Figure 12a). The addition of acid clearly caused an increase in particle size which made the PbS peaks visible (Figure 12b−f), indicating crystallite sizes between 10 and 15 nm (calculated using the Scherrer equation). The absorption spectra lost their exciton features upon addition of acid, probably due to a broadening of the size distribution. Surfactants and hydrochloric acid were also added to the synthesis, but they did not result in particle size changes or absorption edge shifts.

2.1.4.2. Ex Situ Semiconductor Capping. In further efforts to control semiconductor particle sizes and size distributions, capping methods have been developed. Capping agents are typically thiols or mercaptans, which can compete with sulfur (or other counterions) for Pb^{2+} or Cd^{2+} surfaces. In doing so, the capping agent to sulfur ratio chemically determines the particle size. In addition to controlling the particle size, the capping agents act as a surface treatment for the particles which may aid their dispersion into various matrix materials. In these experiments, the particles are prepared ex situ and then dispersed in a polymer matrix to form nanocomposites.

Figure 13 shows the formation of the capped particles schematically. Typically, the sulfide (or other counterions) and capping agent (RS^-) ions are mixed in solution. A solution containing the metal ions is added and semiconductor particles form with sizes determined from the S^{2-}/RS^- ratio. The resulting particles can be studied in solution or can be dried to a powder. By redispersing the capped particles in a polymer solution, nanocomposites can be formed.

Early work in this area focused on colloidal syntheses with no effort to form composites.[78−82] Several thiols were studied and found to control particle size with respect to the ratio of capping agent to counterion in the system. Researchers at DuPont synthesized CdS particles which were capped with thiophenol.[46,83] Using X-ray diffraction and absorbance measurements, they showed that the ratio of capping agent to sulfur chemically controlled the particle size. The nonlinearity of these clusters was measured by third harmonic generation.[84] χ^3 increased from 4.7×10^{-12} esu for a 7 Å molecular cluster to 3.2×10^{-10} esu for 30 Å clusters. Further characterization of these particles included capped precursor synthesis[85] and inelastic neutron-scattering studies.[86]

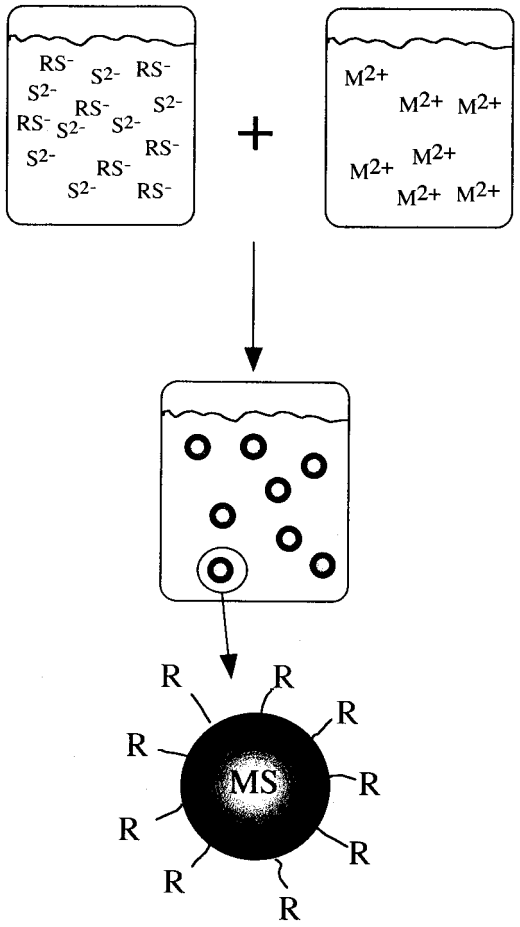

Figure 13. Schematic of ex situ capped semiconductor (MS) synthesis. RS^- is the capping agent, S^{2-} is the sulfur, and M^{2+} is the metal ion.

Some work has been done incorporating the capped particles in polymer matrix materials. Majetich and Carter reported the synthesis of colloidal CdSe capped with six different terminating ligands to study surface effects.[4] Samples were prepared for optical measurements by dispersing the colloids in solid epoxy or poly(methyl methacrylate) matrix materials. The bandgap, absorption oscillator strength, and spectral hole width and trapping time were unaffected by the various surfaces tested. However, the optical hole-burning and luminescence experiments were affected by the surfaces of the particles. Absorption spectra showed excitonic features, indicating a small size distribution in the particles. Nonlinear optical measurements indicated very promising χ^3 values ranging from 6.5×10^{-8} to 2.9×10^{-7} esu (α_2, 8.7×10^{-6} to 1.2×10^{-5} cm/W).

Our group has studied capping syntheses for PbS particles for composite applications.[35] Thiophenol and several other thiols have been investigated as possible capping agents to control particle size as well as tailor the particle surfaces for dispersion into a matrix. All capping systems show the expected Scherrer line broadening in X-ray diffraction studies. Preliminary work has begun on redispersing the capped particles in polymer matrix materials for composite applications.

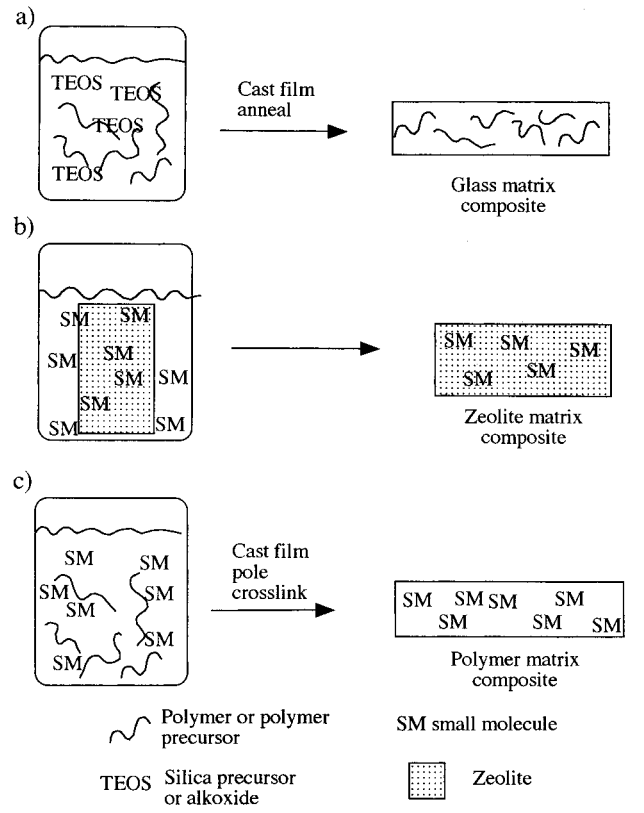

Figure 14. Schematic of composite synthesis with optically active polymers and small molecules. (a) Glass matrix, (b) zeolite matrix, (c) polymer matrix.

2.2. Nanocomposites Containing Polymers and Small Molecules. Many polymers and small molecules exhibit interesting optical effects including second (χ^2) and third (χ^3) order nonlinearities and laser properties. Using the nanocomposite structure, polymers and small molecules such as these can be incorporated into glass, ceramic, and polymer matrix materials as shown in Figure 14. The matrix material can stabilize the compounds, improve the optical properties, and improve the processability as well.

2.2.1. Third-Order Nonlinear Optical Polymers in Glasses. Prasad and co-workers have presented several papers concerning poly(*p*-phenylenevinylene) (PPV) in silica and V_2O_5 matrix materials. PPV is a conjugated polymer with a fast χ^3 nonlinear optical response; however, it shows high optical losses when used in the bulk. Silica and V_2O_5 both show excellent photonic properties, in particular low losses, and improve the optical properties of the PPV when they are combined in a composite. The composite preparation is shown schematically in Figure 14a.

Initial work with silica glass matrixes showed that composites exhibited good optical quality.[87] The UV−vis spectrum of the PPV composite showed a slight blue-shift compared to bulk PPV indicating that the conjugation length was reduced in the composite. The same group performed a study of the NLO response in PPV−silica composites using degenerate four-wave mixing and optical Kerr gate techniques.[88]

Using similar composites, with V_2O_5 instead of silica, two-dimensional gratings were produced by introducing refractive index changes or surface relief patterns with a laser.[89] Gratings such as these could be useful in laser-array systems and multichannel optical communications. A later report on V_2O_5 composites showed that this matrix resulted in a longer conjugation length than seen in the silica composites.[8] The measured χ^3 values were 3×10^{-10} esu for PPV/silica and 6×10^{-10} esu for PPV/V_2O_5, showing a slight improvement in the V_2O_5 system.

2.2.2. Small Molecules in Glasses and Ceramics. Glass and ceramic matrixes can improve the optical, mechanical, and thermal properties of small molecules as discussed in the review by Levy and Esquivas.[70] The synthesis of small molecule glass composites is very similar to that shown in 14a, except that the polymer is replaced with small molecules. Early work in the area of small molecules in glass was reported by Avnir et al. for rhodamine 6G/silica composites.[90] Rhodamine 6G is a laser dye which displays fluorescence, absorption, and emission in the visible region between 500 and 600 nm. This dye is typically used in solution and has problems with concentration quenching and photostability. Many virtues of glass-based composites over solutions include the removal of intermolecular interactions between dye molecules, isolation of impurities, isolation from surrounding atmosphere, good thermal and photostability, and good optical properties among others. Several other laser dyes have also been successfully incorporated into sol−gel derived matrix materials and retained their optical properties.[91] The effect of the dyes on the sol−gel synthesis has been studied.

A significant amount of work has been done incorporating enzymes and other proteins in sol−gel materials.[92,93] Several papers have focused on optical applications of these composites. Bacteriorhodopsin is a light-transducing protein which could be useful as an active component in optically coupled devices. After encapsulation in sol−gel silica glass, the optical and photocycle behavior was retained.[94] This material may also be useful as an optically based ion-sensor. Similar composites were reported which were potentially useful as a real-time holographic medium.[95]

Another light-transducing protein, phycoerythrin, has also been incorporated into sol−gel silica glass.[96] Absorption and fluorescence measurements of the composite showed that the protein retained its optical properties in the matrix and even showed enhanced stability toward photodegradation. Figure 15 shows that the optical properties were retained in the composite by comparing the absorption at several stages in the sol−gel process (Figure 15a−c) to the optical properties in solution (Figure 15d). Only a slight change in the intensity of the peaks at 565 and 495 nm can be identified. The fluorescence spectra are also unchanged with the addition of the matrix, and the material can exhibit two-photon fluorescence. Possible applications of the material include biosensors, 3D biomolecular imaging, and 3D optical storage.

Zeolites have been examined as potential hosts for small molecules with second-order nonlinearities.[97] Composites were prepared as shown in Figure 14b, where the small molecule was vaporized to infiltrate the zeolite. These studies have shown that noncentrosymmetric hosts were necessary to retain the χ^2 properties in the small molecules and in some cases the χ^2 properties were enhanced by the zeolite matrix. The structure of the small molecules in the zeolite host was discussed. The composites can be tuned by changing

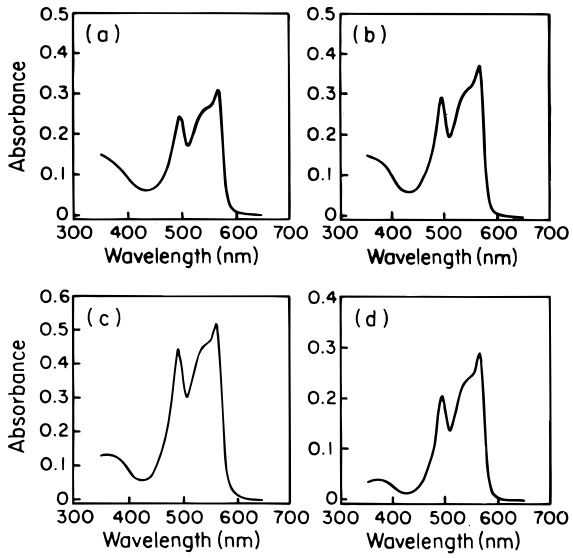

Figure 15. Absorption spectra of phycoerythrin in sol−gel glass at several stages of the sol−gel process (a−c) and in solution (d). Reprinted with permission from ref 96.

the loading level, changing the small-molecule structure, and changing the host framework.

2.2.3. Small Molecules with Second-Order Nonlinearities in Polymer Matrixes. Tripathy et al. have been leaders in the study of small molecules with χ^2 nonlinearity embedded in various high-T_g, cross-linkable polymer matrixes. Several variations of matrixes and small molecules have been studied. As shown in Figure 14c, after mixing the polymer and small molecules, the composites were poled during the cross-linking and cooling procedures to lock in alignment of the χ^2 molecules. In some cases the NLO chromophore could react with the matrix to further lock in orientation. While these hybrids are not true composites since they are largely single-phase materials, they share many features of optical composites.

One example of a system in which the matrix and chromophore interact involves an epoxy-based NLO polymer and a small-molecule NLO chromophore that has been functionalized to be chemically reactive with the epoxy.[98] By photo-cross-linking in the poled state, the optical nonlinearity is stabilized, even at 100 °C. Similar results were found for an alkoxysilane dye, which was incorporated into a siloxane-based host polymer.[99,100] In this case, the host polymer could be cross-linked and could incorporate the dye using sol−gel chemistry. The stability of the χ^2 response at 100 °C was discussed.

Polyimides were also studied as matrix materials for NLO dyes because of their low dielectric constant, ease of processing, and high-temperature stability.[101] Figure 16 shows the stability of the second harmonic coefficient of such a composite at both room temperature and 120 °C. In this case the NLO dye was incorporated into the polyimide using sol−gel chemistry. The composite was quite stable at room temperature; however, it showed a slight loss of χ^2 strength at 120 °C. This result is similar to all of the composites discussed in this section. Finally, NLO active chromophores have been incorporated into hexakis(methoxymethyl)melamine matrix materials.[102] The melamine matrix shows good transparency and high T_g and can be cross-linked using sol−gel chemistry. The resulting composites are slightly less

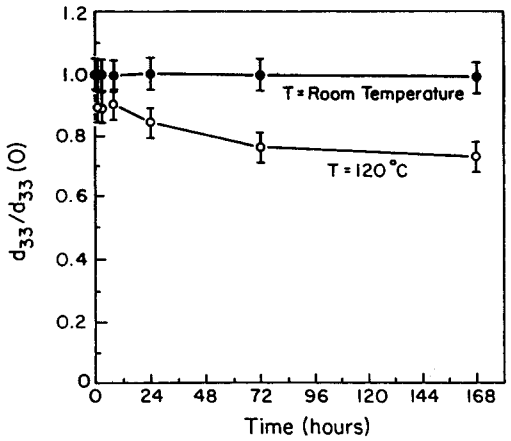

Figure 16. Time behavior of the second harmonic coefficient of a polyimide−small molecule composite. Reprinted with permission from ref 101.

stable than those shown in Figure 16 but show low optical losses.

3. Nanocomposites with Laser Amplification Properties

Using the optical composite principles, our group has developed a method to use the nanocomposite structure to create films with solid-state laser properties.[103,104] By synthesizing composites, the cumbersome process of single-crystal growth typically used for solid-state lasers can be avoided. Additionally, they can be processed as technologically useful films or fibers instead of as monolithic materials. This type of structure may be very important for optical communications applications.

The solid-state laser material our group has focused on is chromium-doped forsterite (Cr−Mg_2SiO_4). In the form of a single crystal, this material has shown tunable lasing in the technologically attractive near-IR region (1167−1345 nm).[105] 1300 nm is a particularly important wavelength in optical communications because it is a dispersion minimum for silica waveguide materials. However, no solid-state laser amplifiers for 1300 nm are currently available. Using the nanocomposite structure, we have developed laser amplifying films that contain Cr forsterite.

Unlike the bulk of the work with semiconductors, our composites are prepared ex situ, with much larger particle sizes (~100 nm), which require tailored refractive index matrix materials to avoid significant scattering. Three steps used in this nanocomposite synthesis are outlined in Figure 17. First, small particles of forsterite were prepared using a dispersion-polymerized prepolymer.[106] The polymer was based on silicon- and magnesium-containing methacrylate monomers, which were randomly copolymerized resulting in 100−500 nm size beads. The beads acted as size templates as they were heated to 1000 °C to remove the organics and crystallize the forsterite. The resulting forsterite particles were about 100 nm in size.

Second, a polymeric matrix material was prepared with the average refractive index of forsterite (1.652 at 589.3 nm).[107] Aromatic and brominated monomers were used to attain this high RI. Several copolymer systems were studied as potential matrix materials, but the most successful was the tribromostyrene/naphthyl methacrylate system. The refractive index could easily be fixed

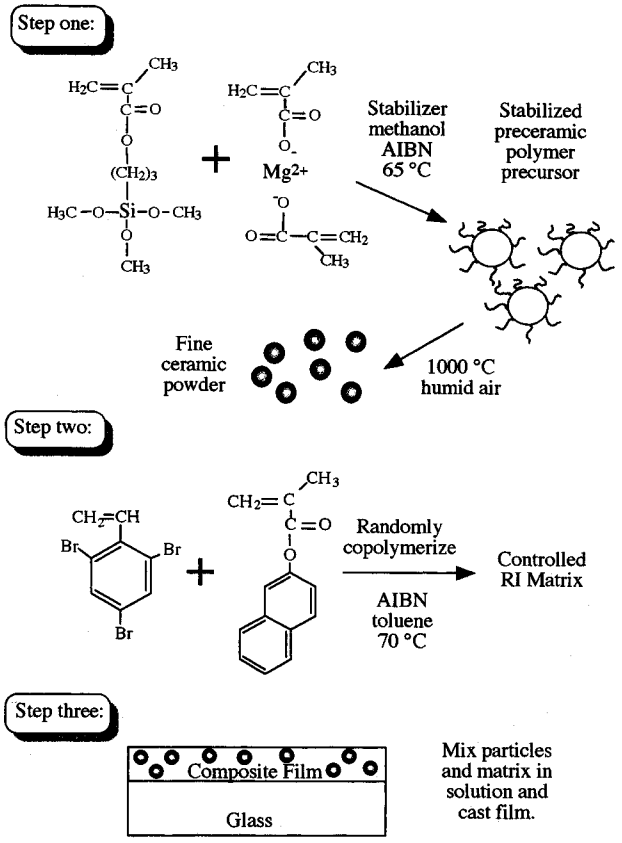

Figure 17. Schematic of ex situ optical composite synthesis for laser amplifying films.

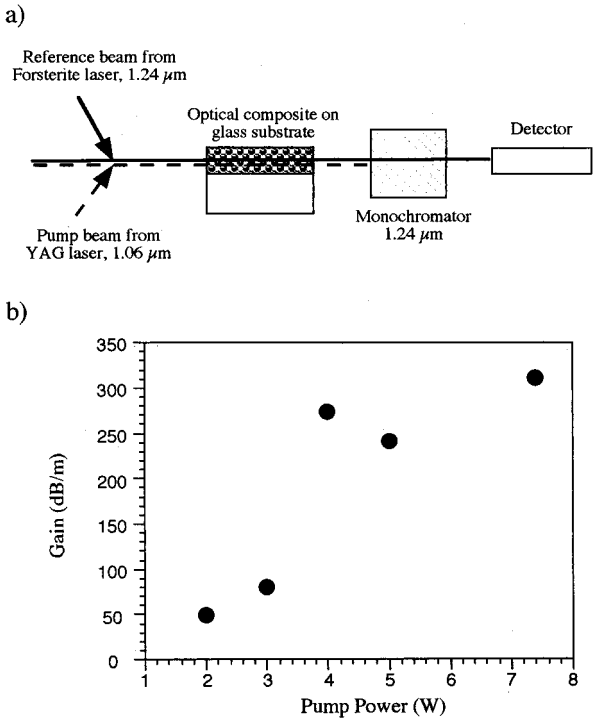

Figure 18. (a) Schematic of the amplification experiment. (b) Amplification in a Cr forsterite nanocomposite as a function of pump power. Reprinted with permission from ref 104.

to 1.65 by the composition of the copolymer, and the material showed good near-IR transparency and good film-forming properties. Finally, the matrix and particles were mixed, and a film was cast on a glass substrate. Typical film dimensions were 2 cm long, 1 cm wide, and 5 μm thick.

Optical measurements were performed on the composite films to examine amplification behavior.[1] The experiment consisted of collinear beams of a Cr forsterite reference at 1.24 μm and a Nd−yittrium aluminum garnet pump at 1.06 μm which were passed through the film as shown in Figure 18a. The pump could be blocked independently from the reference, and was removed from the signal using a monochromator. By comparing the detected signal at the reference wavelength before and during pumping of the sample, a 2-fold increase in signal was observed. Figure 18b shows the relationship between amplification and pump power for these composites. The gain of 300 dB/m exceeds the gain of single-crystal Cr forsterite as well as Er-doped silica fibers used in optical communications at 1.55 μm, which show a gain of 3 dB/m. Other solid-state laser materials and optically functional ceramics are expected to benefit from composite structures such as these.

Recently our group has extended the particle synthesis and composite construction to another system.[1] Cr diopside ($Cr-CaMgSi_2O_6$) is a material that fluoresces in the near-IR (700−1200 nm); however, a single crystal of this material cannot be prepared due to incongruent melting. Thus the potentially useful solid-state laser properties of this material have not been studied. We have synthesized this material using a method similar to the Cr forsterite synthesis and embedded the particles in a high RI matrix. Optical amplification of 95 dB/m has been measured in these composites from 760 to 810 nm using a Ti sapphire laser as the reference signal and an argon laser as a pump. This particular composite system is an excellent example of how nanocomposites can be used to improve the processability and functionality of a material which otherwise was impossible to use.

4. Practical Applications and Issues

4.1. Real Devices. A limited amount of work has been published on devices based on polymer semiconductor composites including two papers that discuss electroluminescence effects. Colvin et al. prepared light-emitting diodes from a layered CdSe/*p*-phenylenevinylene (PPV) composite.[108] The effects from the polymer could be separated from the CdSe in the diode operation. The very low threshold voltage of 4 V, lower than for PPV alone, caused luminescence from the CdSe from red to yellow (depending on particle size), while larger voltages caused the PPV to luminesce in the green. This is seen in Figure 19 as a change in the shape of the electroluminescence curve with changing voltage. This voltage-tunable light source could have important applications in display technology where the applied voltage could determine the color of a pixel. Three particle diameters were examined.

Dabbousi et al. showed electroluminescence using a homogeneous composite of 5−10% CdSe in poly(vinylcarbazole) and an oxadiazole derivative.[109] Experiments with three particle sizes were performed, with emissions from 530 to 650 nm. The turn-on voltage for these composites was a bit higher, at 13 V. These composites also displayed a voltage dependence on light emission, going from red to white with increased voltage.

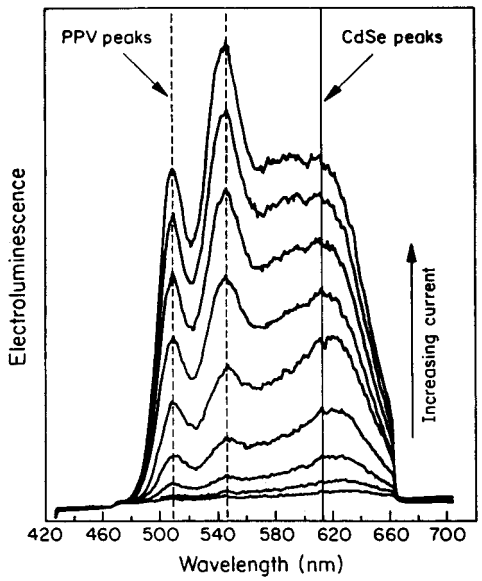

Figure 19. Electroluminescence from a CdSe/PPV composite. Reprinted with permission from ref 108.

4.2. Issues in Nonlinear Optical Composites. Traditional nonlinear optical materials such as barium titanate are difficult to process and integrate into optical applications as they are typically used in single-crystal form. Additionally, stronger nonlinear optical properties are desirable to make these materials technologically useful. Commonly studied semiconductors such as CdS and PbS must be used in the nanocrystal form in order to take advantage of their optical properties as they are opaque in the bulk and the nonlinear optical properties are enhanced at small crystal sizes. Using nanocomposite structures the processability and stability of these materials can be greatly improved. Several issues remain to be solved before these materials will become integrated into mainstream devices.

In quantum-confined semiconductor composites, the particle size and size distributions still need greater control. Enhancement in the optical properties can come only when a very narrow distribution of controlled particle size is used. Additionally, the ability to generate a range of particle sizes in one system is desirable as this would allow operation at many wavelengths. Current techniques are showing improvement in this area, but more is needed to make these materials technologically useful. In systems with polymers and small molecules, stability and processability are key to making useful devices.

4.3. Issues in Optical Amplification with Composites. The area of optically amplifying composites is quite new, and many issues need to be solved before these composites can be integrated into real optical systems. The size of the particles used is very important to the scattering characteristics of the composites. Current techniques discussed here provide laser particles that are larger than would be desirable to avoid all scattering. Additionally the uniformity of the composites must be studied to ensure that the particles are dispersed evenly and without agglomeration in the composites. Finally, the stability of the composites, particularly the polymer matrix materials, must be evaluated. Both prolonged exposure to laser radiation and heat evolution from the laser particles may be issues.

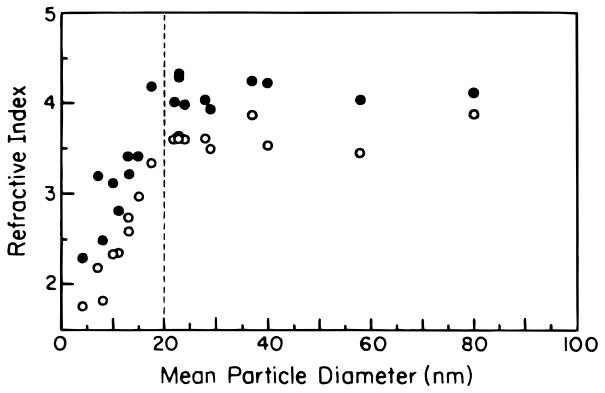

Figure 20. Effects of PbS particle size on the refractive index at 632.8 nm. Nanocomposite values (○), extrapolated values for PbS (●). Reprinted with permission from ref 77.

5. Other Optical Applications

5.1. Composites for High Refractive Index Applications. High refractive index polymers have many applications ranging from antireflection coatings for solar cells to high RI lenses. Our group has synthesized high RI copolymers (up to 1.7) as index-matched matrixes for solid-state laser containing composites (section 3).[107] Semiconductor polymer composites can exhibit even higher refractive indices due to the high RI of the semiconductor phase.

In the work by Zimmerman et al., composites of PbS and gelatin were synthesized and continuously increased the refractive index of the gelatin from 1.5 to 2.5.[110] These materials represented some of the highest refractive index polymers available and were targeted for antireflection coatings for solar cell materials. Kyprianidou-Leodidou et al., from the same research group, varied the size of PbS in poly(ethylene oxide) from 4 to 80 nm by adding surfactants and acids.[77] Again optical measurements were used to evaluate refractive index, showing composite RI values as high as 3.9. As shown in Figure 20, the extrapolated RI of particles greater than 25 nm in size was found to agree with the bulk RI of PbS (4.3). However, the RI was highly dependent on particle size below 20 nm, with 4 nm particles showing a RI of about 2.5. These effects may be due to quantum confinement as strong confinement should become evident at particle sizes near and below 20 nm (Table 2). The absorption of the composites at 632.8 nm decreased as the particle size decreased, also indicating confinement effects. TEM and X-ray were used to characterize the composites and showed broad size distributions.

5.2. Transparent Magnetic Composites. Transparent magnetic materials have many applications including microwave magnetooptical modulation of visible lasers with very low modulation power per unit bandwidth, optical deflection and isolation, magnetooptic displays, and holograms. Usable transparent magnets must have high Curie temperatures, avoid birefringence, and have fundamental absorption edges in the near UV region. The composite structures discussed here may make transparent magnetic materials a reality.

Several groups have prepared magnetic composites with both polymer and glass matrixes. Okada et al. reported the production of sub-100-nm Fe_2O_3 particles in a multibilayer film.[111] Opaque composite films that

contained magnetite behaved as ferromagnets with coercivities of 20 Oe. Papaefthymiou et al. reported magnetic studies of 9−20 nm Fe particles coated with Fe_2O_3 embedded in wax, but the optical properties were not mentioned.[112] Shull et al. prepared Fe^{2+} and Fe^{3+} confined to 20 nm regions in a silica matrix using a sol−gel method.[113] Again the magnetic properties were examined with no mention of transparency. Zhao et al. discussed work embedding colloidal Fe_2O_3 magnetic particles in bilayer lipid membranes.[114] The samples were thin enough to be studied in transmission, but general absorption properties were not measured. Reflective properties and the Kerr and Faraday rotations were examined.

Ziolo et al. reported the production of optically transparent magnetic composites for the first time.[115] γ-Fe_2O_3 was grown in a polymeric ion-exchange resin by introducing the Fe^{3+} and then exposing to H_2O_2 at 60 °C, very similar to the process for preparing CdS in Nafion shown in Figure 3 (steps 1b, 2c). The particles created ranged from 50 to 250 Å in size, which resulted in superparamagnetic properties. If the ionomer resin were loaded multiple times, the particle size did not increase but the concentration of particles did. The composites showed appreciable magnetization at and below room temperature. The highest saturation moment observed was 46 emu/g for 250 Å particles, which is considerably stronger than transparent crystals of $FeBO_3$ (3 emu/g) and FeF_3 (1 emu/g). The absorption coefficient was nearly an order of magnitude less than the bulk crystal, and the composite had a refractive index of 1.6.

Clement et al. presented very promising results for a material which exhibits both χ^2 nonlinearity and magnetic properties.[116] This was accomplished by intercalating a χ^2 small molecule into a ferrimagnetic layered material. The χ^2 response showed very high efficiency, and the magnetic properties could be seen below 40 K. Miller has also outlined many potential applications for molecular/organic magnets.[117]

5.3. Hard Transparent Coatings. By combining the strength and hardness of ceramics with the processability and ductility of polymers, novel transparent materials have been synthesized. Typically these materials are prepared using an in situ synthesis like that shown in Figure 14a. The polymer (or polymer precursor) and silica precursor (or other alkoxide) are mixed in solution and cast as a film or monolith which is subsequently heated to convert the precursors to their final form. Hard transparent coatings and barrier layers are the primary applications of polymer nanocomposites prepared with reinforcing ceramic phases. A significant amount of work in this area has been with polyimide−silica hybrid materials which have high thermal stability, toughness, and hardness.

Our group at Cornell has investigated silica/polyimide materials that show improved hardness and modulus while retaining transparency.[118] The hybrids are based on two different silicon-containing poly(amic acids) (PAA) which are mixed with the silica in situ using sol−gel chemistry. The poly(amic acids) are tailored to be chemically reactive with the silica network. One PAA contains a short siloxane segment which can be cleaved to chemically bond with the silica as it forms. The other PAA is end functionalized with ethoxy groups which can participate in the sol−gel chemistry.

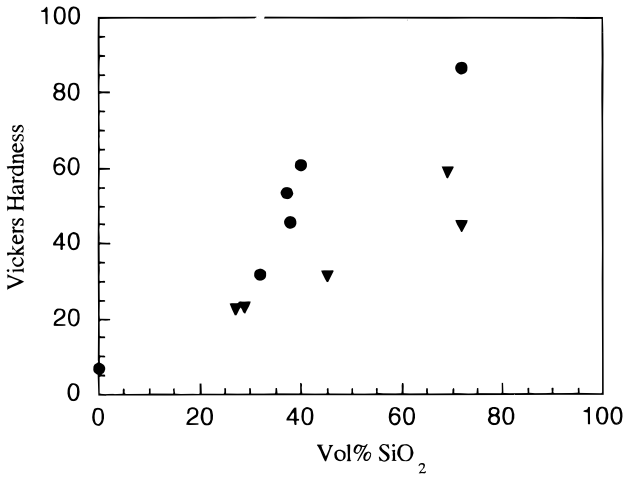

Figure 21. Hardness of siloxane containing (●) and end functionalized (▲) hybrids as a function of silica content. Reprinted with permission from ref 119.

The hybrids formed extremely small silica domains as shown by SEM studies.[119] As expected, the hardness of both types of hybrid increased with increasing silica content as shown in Figure 21. A 17-fold increase in hardness was observed for the siloxane-containing hybrids. The modulus of the hybrids was also improved with increasing silica content. Other work in the area of polyimide−silica hybrids has confirmed that chemical reactivity between phases improves homogeneity of the resulting materials.[120,121]

6. Conclusions and Prospects

Nanocomposite structures based on embedded functional materials in processable matrixes have many optical applications. Particulate phases can be prepared in situ or ex situ and may have properties ranging from laser amplification to improved hardness. Matrix materials can be polymers, glasses, or ceramics. Composites such as these have been used to prepare materials with nonlinear optical properties, laser properties, magnetic properties, and those with high refractive index.

Semiconductor particles have a wealth of optical functions and can be prepared in polymers, ceramics, and glasses. Of particular interest are their third-order nonlinear optical properties, which may be useful for all optical switches. By processing in film or fiber forms, utilizing a composite structure, these devices will be more easily integrated into targeted applications. Composites containing optical polymers and small molecules find advantages over the bulk materials in stability and processability. Solid-state laser materials show great promise as amplifying films in the near-IR and beyond. Finally, novel transparent magnetic materials have also been synthesized using nanocomposite principles and have prospects in printing, data storage, and magnetooptics.

Acknowledgment. L.L.B. is grateful to the National Science Foundation, Department of Education, and Cornell Materials Science Center for support of this research. Eric Kutcher participated in the PbS/PVA

composite studies. Todd Krauss and Inuk Kang have contributed to useful discussions.

References

(1) Beecroft, L. L. *Advanced Nanocomposite Materials for Optical Applications*, Ph.D. Thesis, Cornell University Department of Materials Science and Engineering, 1996; Chapter 4.
(2) Hillinski, E. F.; Lucas, P. A.; Wang, Y. *J. Chem. Phys.* **1988**, *89*, 3435.
(3) Wang, Y.; Suna, A.; McHugh, J.; Hillinski, E. F.; Lucas, P. A.; Johnson, R. D. *J. Chem. Phys.* **1990**, *92*, 6927.
(4) Majetich, S. A.; Carter, A. C. *J. Phys. Chem.* **1993**, *97*, 8727.
(5) Krauss, T. D.; Wise, F. W. *Appl. Phys. Lett.* **1994**, *65*, 1739.
(6) Jain, R. K.; Lind, R. C. *J. Opt. Soc. Am.* **1983**, *73*, 647.
(7) Nogami, M.; Nakamura, A. *Phys. Chem. Glasses* **1993**, *34*, 109.
(8) Wung, C. J.; Wijekoon, W. M. K. P.; Prasad, P. N. *Polymer* **1993**, *34*, 1174.
(9) Justus, B. L.; Tonucci, R. J.; Berry, A. D. *Appl. Phys. Lett.* **1992**, *61*, 3151.
(10) Adair, R.; Chase, L. L.; Payne, S. A. *J. Opt. Soc. Am. B* **1987**, *4*, 875.
(11) Weller, H. *Adv. Mater.* **1993**, *5*, 88.
(12) Alivisatos, A. P. *Science* **1996**, *271*, 933.
(13) Pepper, D. M. *Sci. Am.* **1986**, *254*, 74.
(14) Stegeman, G. I.; Seaton, C. T. *J. Appl. Phys.* **1985**, *58*, R57.
(15) Brus, L. E. *IEEE J. Quantum Electron.* **1986**, *QE-22*, 1909.
(16) Steigerwald, M. L.; Brus, L. E. *Annu. Rev. Mater. Sci.* **1989**, *19*, 471.
(17) Steigerwald, M. L.; Brus, L. E. *Acc. Chem. Res.* **1990**, *23*, 183.
(18) Wang, Y. *Acc. Chem. Res.* **1991**, *24*, 133.
(19) Wang, Y.; Herron, N. *Res. Chem. Intermediates* **1991**, *15*, 17.
(20) Wang, Y.; Herron, N. *J. Phys. Chem.* **1991**, *95*, 525.
(21) Sipe, J. E.; Boyd, R. W. *Phys. Rev. A* **1992**, *46*, 1614.
(22) Boyd, R. W.; Sipe, J. E. *J. Opt. Soc. Am. B* **1994**, *11*, 297.
(23) Boyd, R. W.; Sipe, J. E. *Non-Linear Optics and Optical Physics*; Khoo, I. C., Lam, J. F., Simoni, F., Eds.; World Scientific: Singapore, 1994; p 104.
(24) Fischer, G. L.; Boyd, R. W.; Gehr, R. J.; Jenekhe, S. A.; Osaheni, J. A.; Sipe, J. E.; Weller-Brophy, L. A. *Phys. Rev. Lett.* **1994**, *74*, 1871.
(25) Banyai, L.; Hu, Y. Z.; Lindberg, M.; Koch, S. W. *Phys. Rev. B* **1988**, *38*, 8142.
(26) Ozin, G. A.; Kirkby, S.; Meszaros, M.; Ozkar, S.; Stein, A.; Stucky, G. D. *Materials for Nonlinear Optics*; Marder, S. R., Sohn, J. E., Stucky, G. D., Eds.; American Chemical Society: Washington, DC, 1991; Vol. 455, p 554.
(27) PbS, PbSe, and CdSe values calculated by Inuk Kang.
(28) Wang, Y.; Suna, A.; Mahler, W.; Kasowski, R. *J. Chem. Phys.* **1987**, *87*, 7315.
(29) Nenadovic, M. T.; Comor, M. I.; Vasic, V.; Micic, O. I. *J. Phys. Chem.* **1990**, *94*, 6390.
(30) Alivisatos, A. P.; Harris, A. L.; Levinos, N. J.; Steigerwald, M. L.; Brus, L. E. *J. Chem. Phys.* **1988**, *89*, 4001.
(31) Kuczynski, J. P.; Milosavljevic, B. H.; Thomas, J. K. *J. Phys. Chem.* **1984**, *88*, 980.
(32) Ohtani, B.; Adzuma, S.; Nishimoto, S.; Kagiya, T. *J. Polym. Sci., Part C: Polym. Lett.* **1987**, *25*, 383.
(33) Mahler, W. *Inorg. Chem.* **1988**, *27*, 435.
(34) Gallardo, S.; Gutierrez, M.; Henglein, A.; Janata, E. *Ber. Bunsen-Ges. Phys. Chem.* **1989**, *93*, 1080.
(35) Beecroft, L. L. *Advanced Nanocomposite Materials for Optical Applications*, Ph.D. Thesis, Cornell University Department of Materials Science and Engineering, 1996; Chapter 6.
(36) Berry, C. R. *Phys. Rev.* **1967**, *161*, 848.
(37) Heinglein, A. *Ber. Bunsen-Ges. Phys. Chem.* **1982**, *86*, 301.
(38) Ramsden, J. J.; Gratzel, M. *J. Chem. Soc., Faraday Trans. 1* **1984**, *80*, 919.
(39) Kalyanasundaram, K.; Borgarello, E.; Duonghong, D.; Gratzel, M. *Angew. Chem., Int. Ed. Engl.* **1981**, *20*, 987.
(40) Akimov, I. A.; Denisyuk, I. Yu.; Meshkov, A. M. *Opt. Spectrosc.* **1992**, *72*, 558.
(41) Meissner, D.; Memming, R.; Kastening, B. *Chem. Phys. Lett.* **1983**, *96*, 34.
(42) Krishnan, M.; White, J. R.; Fox, M. A.; Bard, A. J. *J. Am. Chem. Soc.* **1983**, *105*, 7002.
(43) Mau, A. W.; Huang, C.; Kakuta, N.; Bard, A. J.; Campion, A.; Fox, M. A.; White, J. M.; Webber, S. E. *J. Am. Chem. Soc.* **1984**, *106*, 6537.
(44) Wang, Y.; Mahler, W. *Opt. Commun.* **1987**, *61*, 233.
(45) Wang, Y.; Suna, A.; Mahler, W. *Mater. Res. Soc. Symp. Proc.* **1988**, *109*, 187.
(46) Wang, Y.; Herron, N.; Mahler, W.; Suna, A. *J. Opt. Soc. Am. B* **1989**, *6*, 808.
(47) Ohashi, Y.; Ito, H.; Hayashi, T.; Nitta, A.; Matsuda, H.; Okada, S.; Nakanishi, H.; Kato, M. *Springer Proc. Phys.* **1989**, *36*, 81.
(48) Weller, H. *Angew. Chem., Int. Ed. Engl.* **1996**, *35*, 1079.
(49) Murray, C. B.; Kagan, C. R.; Bawendi, M. G. *Science* **1995**, *270*, 1335.
(50) Sankaran, V.; Cummins, C. C.; Schrock, R. R.; Cohen, R. E.; Silbey, R. J. *J. Am. Chem. Soc.* **1990**, *112*, 6858.
(51) Cummins, C. C.; Schrock, R. R.; Cohen, R. E. *Chem. Mater.* **1992**, *4*, 27.
(52) Sankaran, V.; Yue, J.; Cohen, R. E.; Schrock, R. R.; Silbey, R. J. *Chem. Mater.* **1993**, *5*, 1133.
(53) Tassoni, R.; Schrock, R. R. *Chem. Mater.* **1994**, *6*, 744.
(54) Möller, M. *Synth. Met.* **1991**, *41*−*43*, 1159.
(55) Spatz, J. P.; Roescher, A.; Möller, M. *Adv. Mater.* **1996**, *8*, 337.
(56) Yuan, Y.; Cabasso, I.; Fendler, J. *Macromolecules* **1990**, *23*, 3198.
(57) Yuan, Y.; Fendler, J.; Cabasso, I. *Chem. Mater.* **1992**, *4*, 312.
(58) Warnock, J.; Awschalom, D. D. *Phys. Rev. B* **1985**, *32*, 5529.
(59) Cullen, T. J.; Ironside, C. N.; Seaton, C. T.; Stegeman, G. I. *Appl. Phys. Lett.* **1986**, *49*, 1403.
(60) Roussignol, P.; Ricard, D.; Rustagi, K. C.; Flytzanis, C. *Opt. Commun.* **1985**, *55*, 143.
(61) Roussignol, P.; Ricard, D.; Lukasik, J.; Flytzanis, C. *J. Opt. Soc. Am. B* **1987**, *4*, 5.
(62) Borelli, N. F.; Hall, D. W.; Holland, H. J.; Smith, D. W. *J. Appl. Phys.* **1987**, *61*, 5399.
(63) Sombra, A. S. B. *Solid State Commun.* **1992**, *82*, 805.
(64) Kuczynski, J.; Thomas, J. K. *J. Phys. Chem.* **1985**, *89*, 2720.
(65) Luong, J. C. *Superlattices Microstruct.* **1988**, *4*, 385.
(66) Wang, Y.; Herron, N. *J. Phys. Chem.* **1987**, *91*, 257.
(67) Herron, N.; Wang, Y.; Eddy, M. M.; Stucky, G. D.; Cox, D. E.; Moller, K.; Bein, T. *J. Am. Chem. Soc.* **1989**, *111*, 530.
(68) Wang, Y.; Herron, N. *J. Phys. Chem.* **1988**, *92*, 4988.
(69) Moller, K.; Bein, T.; Herron, N.; Mahler, W.; Wang, Y. *Inorg. Chem.* **1989**, *28*, 2914.
(70) Levy, D.; Esquivias, L. *Adv. Mater.* **1995**, *7*, 120.
(71) Rajh, T.; Vucemilovic, M. I.; Dimitrijevic, N. M.; Micic, O. I.; Nozik, A. J. *Chem. Phys. Lett.* **1988**, *143*, 305.
(72) Nogami, M.; Nagasaka, K.; Takata, M. *J. Non-Cryst. Solids* **1990**, *122*, 101.
(73) Nogami, M.; Nagaska, K.; Kato, E. *J. Am. Ceram. Soc.* **1990**, *73*, 2097.
(74) Othmani, A.; Bovier, C.; Dumas, J.; Champagnon, B. *J. Phys. IV* **1992**, *2*, C2−275.
(75) Nogami, M.; Kato, A.; Tanaka, Y. *J. Mater. Sci.* **1993**, *28*, 4129.
(76) Danek, M.; Jensen, K. F.; Murray, C. B.; Bawendi, M. G. *J. Cryst. Growth* **1994**, *145*, 714.
(77) Kyprianidou-Leodidou, T.; Caseri, W.; Suter, U. *J. Phys. Chem.* **1994**, *98*, 8992.
(78) Nosaka, Y.; Yamaguchi, K.; Miyama, H.; Hayashi, H. *Chem. Lett.* **1988**, 605.
(79) Steigerwald, M. L.; Alivisatos, A. P.; Gibson, J. M.; Harris, T. D.; Kortan, R.; Muller, A. J.; Thayer, A. M.; Duncan, T. M.; Douglass, D. C.; Brus, L. E. *J. Am. Chem. Soc.* **1988**, *110*, 3046.
(80) Fischer, C.; Heinglein, A. *J. Phys. Chem.* **1989**, *93*, 5578.
(81) Swayambunathan, V.; Hayes, D.; Schmidt, K. H.; Liao, Y. X.; Meisel, D. *J. Am. Chem. Soc.* **1990**, *112*, 3831.
(82) Lawless, D.; Kapoor, S.; Meisel, D. *J. Phys. Chem.* **1995**, *99*, 10329.
(83) Herron, N.; Wang, Y.; Eckert, H. *J. Am. Chem. Soc.* **1990**, *112*, 1322.
(84) Cheng, L. T.; Herron, N.; Wang, Y. *J. Appl. Phys.* **1989**, *66*, 3417.
(85) Herron, N.; Suna, A.; Wang, Y. *J. Chem. Soc., Dalton Trans.* **1992**, 2329.
(86) Markichev, I.; Sheka, E.; Natkaniec, I.; Muzychka, A.; Khavryutchenko, V.; Wang, Y.; Herron, N. *Physica B* **1994**, *198*, 197.
(87) Wung, C. J.; Pang, Y.; Prasad, P. N.; Karasz, F. E. *Polymer* **1991**, *32*, 605.
(88) Pang, Y.; Samoc, M.; Prasad, P. N. *J. Chem. Phys.* **1991**, *94*, 5282.
(89) He, G. S.; Wung, C. J.; Xu, G. C.; Prasad, P. N. *Appl. Opt.* **1991**, *30*, 3810.
(90) Avnir, D.; Levy, D.; Reisfeld, R. *J. Phys. Chem.* **1984**, *88*, 5956.
(91) Haruvy, Y.; Webber, S. E. *Chem. Mater.* **1991**, *3*, 501.
(92) Avnir, D.; Braun, S.; Lev, O.; Ottolenghi, M. *Chem. Mater.* **1994**, *6*, 1605.
(93) Ellerby, L. M.; Nishida, C. R.; Nishida, F.; Yamanaka, S. A.; Dunn, B.; Valentine, J. S.; Zink, J. I. *Science* **1992**, *255*, 1113.
(94) Wu, S.; Ellerby, L. M.; Cohan, J. S.; Dunn, B.; El-Sayed, M. A.; Valentine, J. S.; Zink, J. I. *Chem. Mater.* **1993**, *5*, 115.
(95) Weetall, H. H.; Robertson, B.; Cullin, D.; Brown, J.; Walch, M. *Biochim. Biophys. Acta* **1993**, *1142*, 211.
(96) Chen, Z.; Samuelson, L. A.; Akkara, J.; Kaplan, D. L.; Gao, H.; Kumar, J.; Marx, K. A.; Tripathy, S. K. *Chem. Mater.* **1995**, *7*, 1779.
(97) Cox, S. D.; Gier, T. E.; Stucky, G. D. *Chem. Mater.* **1990**, *2*, 609.
(98) Jeng, R. J.; Chen, Y. M.; Kumar, J.; Tripathy, S. K. *J. Macromol. Sci.—Pure Appl. Chem.* **1992**, *A29*, 1115.
(99) Jeng, R. J.; Chen, Y. M.; Jain, A. K.; Kumar, J.; Tripathy, S. K. *Chem. Mater.* **1992**, *4*, 972.
(100) Jeng, R. J.; Chen, Y. M.; Jain, A. K.; Tripathy, S. K.; Kumar, J. *Opt. Commun.* **1992**, *89*, 212.
(101) Jeng, R. J.; Chen, Y. M.; Jain, A. K.; Kumar, J.; Tripathy, S. K. *Chem. Mater.* **1992**, *4*, 1141.

(102) Jeng, R. J.; Hsiue, G. H.; Chen, J. I.; Marturunkakul, S.; Li, L.; Jiang, X. L.; Moody, R. A.; Masse, C. E.; Kumar, J.; Tripathy, S. K. *J. Appl. Polym. Sci.* **1995**, *55*, 209.
(103) Beecroft, L. L.; Barber, D. B.; Mass, J. L.; Burlitch, J. M.; Pollock, C. R.; Ober, C. K. *ACS Div. Polym. Mater.: Sci. Eng.* **1995**, *73*, 162.
(104) Beecroft, L. L.; Leidner, R. T.; Ober, C. K.; Barber, D. B.; Pollock, C. R. *Better Ceramics Through Chemistry VII*; Wilkes, G. L., Schaefer, D. W., Sanchez, C., Coltrain, B., Eds.; *Mater. Res. Soc. Symp. Proc.* **1996**, *435*, 575.
(105) Petricevic, V.; Geyen, S. K.; Alfano, R. R.; Yamagishi, K.; Anzai, H.; Yamaguchi, Y. *Appl. Phys. Lett.* **1988**, *52*, 1040.
(106) Beecroft, L. L.; Ober, C. K. *Adv. Mater.* **1995**, *7* (*12*), 1009.
(107) Beecroft, L. L.; Ober, C. K. *J. Macromol. Sci.—Pure Appl. Chem.* **1997**, *A34*, 573.
(108) Colvin, V. L.; Schlamp, M. C.; Alivisatos, A. P. *Nature* **1994**, *370*, 354.
(109) Dabbousi, B. O.; Bawendi, M. G.; Onitsuka, O.; Rubner, M. F. *Appl. Phys. Lett.* **1995**, *66*, 1316.
(110) Zimmerman, L.; Weibel, M.; Caseri, W.; Suter, U. *J. Mater. Res.* **1993**, *8*, 1742.
(111) Okada, H.; Sakata, K.; Kunitake, T. *Chem. Mater.* **1990**, *2*, 89.
(112) Papaefthymiou, V.; Kostikas, A.; Simopoulos, A.; Niarchos, D.; Gangopadyay, S.; Hadjipanayis, G. C.; Sorensen, C. M.; Kablunde, K. J. *J. Appl. Phys.* **1990**, *67*, 4487.
(113) Shull, R. D.; Ritter, J. J.; Shapiro, A. J.; Swartzndruber, L. J.; Bennett, L. H. *J. Appl. Phys.* **1990**, *67*, 4490.
(114) Zhao, X. K.; Herve, P. J.; Fendler, J. H. *J. Phys. Chem.* **1989**, *93*, 908.
(115) Ziolo, R. F.; Gianellis, E. P.; Weinstein, B. A.; O'Horo, M. P.; Ganguly, B. N.; Mehrotra, V.; Russell, M. W.; Huffman, D. R. *Science* **1992**, *257*, 219.
(116) Clement, R.; Lacroix, P. G.; O'Hare, D.; Evans, J. *Adv. Mater.* **1994**, *6*, 794.
(117) Miller, J. S. *Adv. Mater.* **1994**, *6*, 322.
(118) Johnen, N. A.; Beecroft, L. L.; Ober, C. K. *Recent Advances in Step Growth Polymerization*; Hedrick, J., Labadie, J., Eds.; American Chemical Society: Washington, DC, 1995; Vol. 624, p 392.
(119) Beecroft, L. L.; Johnen, N. A.; Ober, C. K. *Polym. Adv. Technol.* **1997**, *8*, in press.
(120) Kakimoto, M.; Iyoku, Y.; Morikawa, A.; Imai, Y. *Polym. Prepr., Proc. ACS Div. Polym Chem.* **1994**, *35* (1), 393.
(121) Morikawa, A.; Iyoku, Y.; Kakimoto, M.; Imai, Y. *J. Mater. Chem.* **1992**, *2*, 679.

CM960441A